Science of the Total Environment 631–632 (2018) 570–579

Contents lists available at ScienceDirect

Science of the Total Environment

journal homepage: www.elsevier.com/locate/scitotenv

Silica nanoparticles promote oxLDL-induced macrophage lipid accumulation and apoptosis via endoplasmic reticulum stress signaling

Caixia Guo [a,b], Ru Ma [a,b], Xiaoying Liu [b,c], Tian Chen [a,b], Yang Li [b,c], Yang Yu [b,c], Junchao Duan [b,c], Xianqing Zhou [b,c], Yanbo Li [b,c,*], Zhiwei Sun [b,c,*]

[a] Department of Occupational Health and Environmental Health, School of Public Health, Capital Medical University, Beijing 100069, China
[b] Beijing Key Laboratory of Environmental Toxicology, Capital Medical University, Beijing 100069, China
[c] Department of Toxicology and Sanitary Chemistry, School of Public Health, Capital Medical University, Beijing 100069, China

HIGHLIGHTS

- SiNPs enhanced oxLDL-induced macrophage lipid accumulation and apoptosis.
- Lipid accumulation was caused through promoting cholesterol influx, inhibiting cholesterol efflux by SiNPs and oxLDL.
- ER stress PERK/eIF2α/ATF4 and IRE1α/XBP1 signaling participated in the adverse effects induced by SiNPs and oxLDL coexposure.

GRAPHICAL ABSTRACT

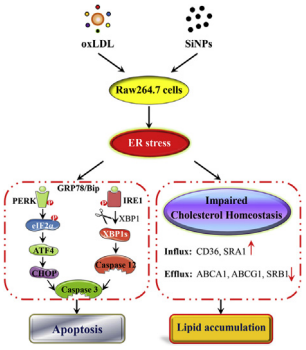

ARTICLE INFO

Article history:
Received 27 September 2017
Received in revised form 26 February 2018
Accepted 26 February 2018
Available online xxxx

Editor: Scott Sheridan

Keywords:
Nanoparticle
Macrophage
Cholesterol
ER stress

ABSTRACT

Oxidized low-density lipoprotein (oxLDL), a marker of hyperlipidemia, plays a pivotal role in the development of atherosclerosis through the induction of macrophage-derived foam cell formation and thereafter apoptosis. Previous studies have indicated that silica nanoparticle (SiNPs) may exert a proatherogenic role, which could induce endothelial dysfunction, and monocytes infiltration. However, little is known about SiNPs' effects on macrophage-derived foam cell formation and apoptosis in the pathogenesis of atherosclerosis. In this study, we investigated the effects of SiNPs and oxLDL coexposure on macrophage-derived lipid metabolism, foam cell and apoptosis by using Raw264.7 cells. As a result, SiNPs enhanced cytotoxicity, apoptosis, and lipid accumulation upon oxLDL stimulation. Furthermore, quantitative determination of the expression levels of genes involved in cholesterol influx or efflux showed significantly up-regulated expressions of CD36 and SRA, whereas down-regulated expressions of ATP-binding cassette A1 (ABCA1), ABCG1, and SRB1 in oxLDL-treated macrophages, especially upon the co-exposure with SiNPs. It indicated that SiNPs promoted lipid accumulation in macrophage cells through not only facilitating cholesterol influx but also inhibiting cholesterol efflux. Endoplasmic reticulum (ER) is specialized for the production, modification, even trafficking of lipids. Interestingly, ER response was triggered upon oxLDL treatment, while SiNPs coexposure augmented the ER stress. Taken together, our results revealed that SiNPs promoted oxLDL-induced macrophage foam cell formation and apoptosis, which may be mediated by ER stress signaling. Thus we propose future researches needed for a better understanding of NPs' toxicity and their interactions with various pathophysiological conditions.

* Corresponding authors at: Department of Toxicology and Sanitary Chemistry, School of Public Health, Capital Medical University, No.10 Xitoutiao, You An Men, Beijing 100069, China.
E-mail addresses: ybli@ccmu.edu.cn (Y. Li), zwsun@ccmu.edu.cn (Z. Sun).

https://doi.org/10.1016/j.scitotenv.2018.02.312
0048-9697/

1. Introduction

There is a global epidemic of cardiovascular disease (CVD), which is also a leading cause of health loss worldwide. According to the Global Burden of Disease Study 2015, there were an estimated 422.7 million cases of CVD and 17.92 million CVD deaths in 2015, which accounted for one-third of all deaths (Roth et al., 2017). Emerging evidence indicated that environmental exposure may also contribute to the global epidemic of CVD and other metabolic consequences. For example, a growing number of epidemiological and experimental studies have provided sufficient evidence for a causal effect of acute/chronic exposure to particulate matter (PM) on the progression of atherosclerosis, and the morbidity and mortality of CVD (Brook et al., 2017). Moreover, nanoscale ultrafine particle (UFP) appears to be more potent in the induction of cardiovascular effects, which may attribute to their relatively smaller size, larger effective surface area, deeper penetration in human airways and probably systemic transportation (Traboulsi et al., 2017).

UFP in which silicon is an important inorganic component, were widely spread in the atmosphere through sandstorm, construction and combustion processes (Asweto et al., 2017). Silica is widely used as model particle for atmospheric studies (Lu et al., 2015). Meanwhile, engineered silica nanoparticles (SiNPs) have been widely used as biosensor, or carriers for gene therapy and drug delivery, which inevitably brings human potential exposure to SiNPs through environmental, occupational and even iatrogenic ways. Interestingly, a recent study provided a more compelling evidence that besides the translocation from lung to systemic circulation, the inhaled NPs preferentially accumulated at sites of vascular inflammation (Miller et al., 2017). Reportedly, SiNPs exposure had pro-atherogenic effects, which disrupted vascular homeostasis (Nemmar et al., 2014), induced endothelial dysfunction (Guo et al., 2015; Guo et al., 2016; Liu and Sun, 2010), promoted inflammation and monocyte-endothelial cell adhesion (Liu et al., 2012; Napierska et al., 2013), and also trigger cytotoxicity, oxidative stress and triglyceride accumulation on macrophage (Petrick et al., 2016). All those evidences revealed SiNPs exposure may promote atherosclerosis. Nevertheless, sadly, our understanding of the health and safety aspects of NPs is still very limited, even highly controversial.

Atherosclerosis is involved in the pathogenesis of CVD. Among the risk factors, dyslipidemia provides a vital role in the occurrence and development of atherosclerosis. Notably, a recent report showed that more than a half (58.72%) of Chinese population suffers from dyslipidemia (Li et al., 2017). Oxidative stress induced by PM or NPs exposure could initiate atheroma development by oxidizing low-density lipoprotein (LDL) (Arai, 2014; Chang et al., 2014), as well as inducing endothelial dysfunction (Guo et al., 2015; Guo et al., 2016). The oxidized LDL (oxLDL) has been considered as a critical risk factor for the initiation and progression of hyperlipidemia, which could increase vascular permeability to serum proteins in an early stage of atherosclerosis (May and Qu, 2010), and also induce macrophage apoptosis contributing to rupture and destabilization of atherosclerotic plaques (Linton et al., 2000). High plasma and plaque levels of oxLDL were closely correlated with CVD and plaque disruption (Nishi et al., 2002).

Atherosclerosis is characterized by the accumulation of macrophages and oxLDL in the intimal layer of elastic and muscular arteries. oxLDL is a well-recognized risk factor for atherosclerosis, directly responsible for exacerbating macrophage activation and atherosclerosis. Macrophages participate in all stages of atherosclerosis, a chronic inflammatory state. It was well-documented that macrophage foam cell formation and apoptosis are crucial determinants of the initiation and progression of atherosclerosis lesion (Linton et al., 2016), which participate in the formation and expansion of lipid core, contributing to plaque instability and rupture (Bobryshev et al., 2016). Up to date, the pro-inflammatory potential of SiNPs on macrophage had been well elucidated (Breznan et al., 2017). However, the influence of these particles on macrophage lipid accumulation and apoptosis is poorly understood. It is well-recognized that SiNPs could enter the vascular system indirectly by inhalation, ingestion or skin contact, and even directly through vein injection (Du et al., 2013; Matsuo et al., 2016; Nemmar et al., 2016). Previous studies had confirmed the recruited monocytes to lesional endothelial cells induced by SiNPs exposure (Liu et al., 2012; Napierska et al., 2013). Similarly to oxLDL, SiNPs could not only induce endothelial injury and dysfunction (Guo et al., 2018), but also directly increase the permeability of vascular endothelium to molecules that would not otherwise cross the barrier (Tay et al., 2017). Interesting, the SiNPs-induced endothelial leakiness even occurred at condition that did not entail increase in intracellular reactive oxygen species (ROS) level nor compromised cell viability (Tay et al., 2017). In view of the increasing vascular exposure of SiNPs, the prevalence of hyperlipidemia and their role in atherosclerosis, there is great possibility for their interaction (SiNPs and oxLDL) with macrophages and to influence atherosclerosis. In this context, this paper was aimed to determine the influence on macrophage lipid accumulation and apoptosis upon oxLDL and SiNPs coexposure, and elucidate the mechanisms behind these adverse effects, which would provide new insights into cardiovascular risks associated with NPs exposure.

2. Materials and methods

2.1. Materials

The amorphous SiNPs were synthesized through the Stöber method by the College of Chemistry, Jilin University, China, and characterized as described in our previous study (Guo et al., 2016). Briefly, 2.5 mL of tetraethylorthosilicate was added to a premixed ethanol solution (50 mL) containing 2 mL of ammonia and 1 mL of water. The mixture was kept stirring (150 rpm) at 40 °C for 12 h and was then centrifuged at 12,000 rpm for 15 min to isolate the particles. After washing with deionized water for three times, the particles were dispersed in 50 mL of deionized water and sterilized by autoclave (0.1 MPa, 120 °C, 20 min) as a concentrated suspension for further experiments. Transmission electron microscope (TEM) (JEOL JEM2100, Japan) was used for assessing the particle size and morphology. The hydrodynamic size of synthesized particles was assessed by dynamic light scattering (DLS) method using a Zetasizer (Malvern Nano-ZS90, UK), and the zeta potential measurements were also done by the same device. Additionally, an inductively coupled plasma atomic emission spectrometry (ICP-AES) (Agilent 720, USA) was performed for purity analysis, and Limulus Amebocyte Lysate (LAL) assay for endotoxin test. Raw264.7, mouse macrophage cell line, was obtained from the Cell Resource Center, Shanghai Institutes for Biological Sciences, China (SIBS, Shanghai, China). oxLDL was purchased from Xiesheng Biotech (Beijing, China). Kits for Annexin V-FITC Apoptosis Detection and lactate dehydrogenase (LDH) determination were purchased from KeyGen Biotech (KeyGen, Nanjing, China), and kit for total cholesterol (TC) measurement from Applygen Technologies Inc. (Applygen, Beijing, China). The primary antibodies for PERK, p-PERK, eIF2α, p-eIF2α, GRP78, CHOP, caspase-3 and GAPDH were all acquired from Cell Signaling Technology, USA, and while the primary antibodies for IRE1α, p-IRE1α, and caspase-12 were from Abcam, USA.

2.2. Cell culture and treatment

Raw264.7 cells were cultured in Dulbecco's modified Eagle's medium (DMEM) (Thermo Fisher Sientific, USA) supplemented with 10% fetal bovine serum (FBS) (Thermo Fisher Sientific, USA) in the cell incubator at 37 °C in a 5% CO_2 humidified environment. Cells were incubated up to about 24 h and grown to about 80% confluence before experiments. SiNPs and oxLDL were diluted to appropriate concentrations by DMEM culture medium. After oxLDL and SiNPs coexposure, cells or media were harvested for a series of measurements according to the experiment schedule.

2.3. SiNPs uptake measurements

The morphological observation of SiNPs' uptake and the further quantification of intracellular SiNPs amount were determined using TEM and ICP-AES, respectively as previously described (Guo et al., 2016).

2.4. Cell viability determination

The conversion of the tetrazolium salt MTT to a colored formazan by mitochondrial dehydrogenase was used to assess cell viability. To noted, the treatment doses of SiNPs were selected according to the reported in vitro cell culture studies about SiNPs (Murugadoss et al., 2017), and also the IC_{50} assessment via MTT assay in our lab. Ultimately, the IC_{50} of SiNPs (24-h exposure to Raw264.7 cells) were about 200 μg/mL (details in Supplementary Fig. S1). Thus the used concentrations of SiNPs in the current study were 1/16, 1/8, 1/4 and 1/2 IC_{50} in turn, that is, 12.5, 25, 50 and 100 μg/mL, respectively. For the detail of MTT assay, firstly, 1×10^4 cells were placed in each of 96 wells. Then cells were treated with 25 μg/mL oxLDL and also SiNPs (12.5, 25, 50 and 100 μg/mL, respectively) for 24 h. After treatment, 10 μL of 5 mg/mL MTT (Sigma, USA) were added to each well and further incubated at 37 °C for 4 h. Then the absorbance was measured at 490 nm using a microplate reader (SpectraMax M5; Molecular Devices, USA).

2.5. Cellular membrane integrity measurement

LDH release assay was used to indicate the injury to cell membrane integrity, consequently resulting in an irreversible cell death. Thus the LDH activity in media was determined using a LDH assay kit according to the manufacturer's protocols. Finally, the amount of LDH released is expressed as LDH activity (U/L) in culture media.

2.6. Apoptosis determination

Cell apoptosis was quantified by flow cytometry (FCM) with FITC-conjugated Annexin V/propidium iodide (PI) double-staining assay, using an Annexin V-FITC Apoptosis Detection Kit according to the manufacturer's instructions. At last, the cells (at least 1×10^4 cells per sample) were subjected to flow cytometer (Becton Dickinson, USA), and percentages of viable and apoptotic cells were determined.

2.7. Intracellular lipid measurement

The intracellular lipid droplets were determined using oil red O staining. Briefly, after oxLDL treatment with or without the presence of SiNPs, cells were washed with phosphate buffered saline (PBS) for three times, and stained with oil red O (0.3%) in isopropanol for 30 min, and then examined under an Olympus IX81 microscope (Tokyo, Japan). Further, the intracellular content of TC was quantified according to the manufacturer's instructions and normalized to the level of total cellular protein.

2.8. Intracellular calcium level detection

The intracellular calcium level was reflected through using the fluorescent calcium indicator, Fluo-3 AM (Beyotime, China) according to our previous study (Guo et al., 2018). Briefly, after treatment, cells were washed with PBS for three times, and then incubated with 5 μmol/L Fluo-3 AM for 20 min. Ultimately, the cells were imaged under a laser scanning confocal microscope, LSCM (LSM 710; Zeiss, Germany).

2.9. Quantitative real-time RT-PCR

Total RNA was extracted from cells using RNAiso Plus (Takara, Japan), and reverse transcribed into cDNA using PrimeScript™ RT Master Mix (Takara, Japan). Real-time quantitative PCR was conducted by using the SYBR Premix Ex Taq™ II (Takara, Japan) in a real-time PCR machine (Eppendorf, Germany). mRNA levels of endoplasmic reticulum (ER) stress- (XBP1U, XBP1S, ATF4, GRP78, HERPUD1, CHOP) and lipid influx/efflux- (CD36, SRA, SRB1, ABCA1 and ABCG1) associated markers were determined. Each experiment was carried out in triplicate with *β-actin* as the internal standard, and primers (*Mus musculus*) for quantitative PCR detection were listed in Table 1.

2.10. Western blot analysis

The Western blot assay was used to detect the expressions of ER stress markers, including PERK, p-PERK, eIF2α, p-eIF2α, IRE1α, p-IRE1α, GRP78, CHOP and caspase-12, and also that of the apoptotic executor, caspase-3. GAPDH was detected as the internal control. At least three independent experiments were performed. Additionally, the photodensitometric analysis of the protein band was performed and quantified by using Image Lab™ Software (Bio-Rad, USA).

2.11. Statistical analysis

All the Data were presented as means ± SD. Student's *t*-test was used for the examination of statistical significance, except for the comparison of "SiNPs intracellular uptake" using one-way analysis of variance (ANOVA) followed by the least significance difference (LSD) test. All comparisons were two-tailed, and statistical significance was set at $P < 0.05$.

3. Results

3.1. SiNPs characterization

TEM micrographs manifested SiNPs were spherical or near-spherical shape, no aggregation but good monodispersibility (Fig. 1). The primary particle size was 57.66 ± 7.30 nm as calculated by Image J software, with a relatively good normal distribution. DLS and zeta potential measurements showed that SiNPs had a hydrodynamic mean particle diameter of 106 nm, a polydispersity index of 0.12, and zeta potential of −34 mV in ultrapure water up to 24 h. The purity analysis confirmed of <0.004% (w:w) of Ca, Mg, Fe, Mn, Al, and Cr. Additionally, no endotoxin was detectable in SiNPs suspensions.

Table 1
Real-time PCR primer pairs.

Gene	Description	Primer sequence
XBP1U	F	TTTGGGCATTCTGGACAAGT
	R	AAAGGGAGGCTGGTAAGGAA
XBP1S	F	CTGAGTCCGCAGCAGGTG
	R	GACCTCTGGGAGTTCCTCCA
ATF4	F	CCTATAAAGGCTTGCGGCCA
	R	GTCCGTTACAGCAACACTGC
GRP78	F	GTGTGTGAGACCAGAACCGT
	R	ACAGTGAACTTCATCATGCCG
HERPUD1	F	AATGCCAGAAACCAGCACA
	R	TTGCCGTAAACCATCACTTG
CHOP	F	CCAGGAAACGAAGAGGAAGA
	R	CTTTGGGATGTGCGTGTG
CD36	F	GTGCTCTCCCTTGATTCTGC
	R	CTCCAAACACAGCCAGGAC
SRA	F	AGTCAGTGGATGGTGGGAGT
	R	GGAAGCCTGGTATTGTCTGG
SRB1	F	GCCTGTTTGTTGGGATGAA
	R	AGTCCGTTCCATTTGTCCAC
ABCA1	F	GGAAGGCACTCAAGCCACT
	R	CAGCCAACTCCTGAAAGGTC
ABCG1	F	TACCTGGATTTCATCGTCCTG
	R	AATGTCTGCTTTGCCTCGTT
β-*actin*	F	GAGACCTTCAACACCCCAGC
	R	ATGTCACGCACGATTTCCC

3.2. SiNPs cellular uptake in Raw264.7 cells

SiNPs cellular uptake was investigated after 24 h' treatment of SiNPs. As manifested in Fig. 2A, the intracellular silicon content in macrophages was increased in a dose-dependent manner. Moreover, in line with the previous study (Hashimoto and Imazato, 2015), TEM image showed the internalized particles were mainly observed in the cell vesicles (as depicted in Fig. 2B).

3.3. SiNPs aggravated oxLDL-induced cytotoxicity in RAW264.7 cells

Results showed the oxLDL treatment (25 μg/mL, 24 h) reduced cell viability by approximately 13.2% as measured using MTT assay. Furthermore, SiNPs (12.5–100 μg/mL) remarkably enhanced the cell viability inhibitory effect induced by oxLDL (Fig. 3A). Next, the cytotoxic effect of SiNPs on RAW264.7 cells was further certified by using LDH leakage assay. As shown in Fig. 3B, LDH release into culture media increased dramatically after oxLDL-treated cells co-incubated with SiNPs. All these indicated that SiNPs aggravated cytotoxicity of Raw264.7 cells induced by oxLDL.

3.4. SiNPs promoted oxLDL-induced apoptosis in RAW264.7 cells

Results showed the oxLDL treatment (25 μg/mL, 24 h) induced apoptosis by approximately 11.1% as measured using FCM, whereas SiNPs cotreatment (100 μg/mL) enhanced oxLDL-induced apoptosis, which increased the apoptotic rate up to 21.0% (Fig. 4A). Since Caspase-3 activation was an indicator of apoptosis, we further determine the expression of cleaved caspase-3. Expectedly, the expression of cleaved caspase-3 was increased after oxLDL treatment, and became higher following the cotreatment of SiNPs and oxLDL (Fig. 4B).

3.5. SiNPs enhanced oxLDL-induced lipid accumulation in RAW264.7 cells

Foam cell formation, a hallmark event of atherosclerosis, can be induced by excess oxLDL. The Oil red staining showed that SiNPs promoted oxLDL-induced lipid accumulation in RAW264.7 cells (as depicted in Fig. 5A). Similarly, as illuminated in Fig. 5B, the intracellular TC content measurement also confirmed a promotion effect of SiNPs on lipid accumulation. Next, we detected the gene expressions of factors involved in cholesterol efflux and influx. Exactly, as manifested in Fig. 5C, the expressions of CD36, SRA were up-regulated, while that of SRB1, ABCA1 and ABCG1 were down-regulated in oxLDL-treated Raw264.7 cells. Moreover, oxLDL-induced gene alterations were significantly enhanced by SiNPs coexposure, suggesting that SiNPs may enhance the lipid accumulation via promoting CD36, SRA expression for cholesterol influx to macrophages, and also via inhibiting SRB1, ABCA1 and ABCG1 to alleviate cholesterol efflux, which consequently resulting in lipid accumulation, even foam cell formation.

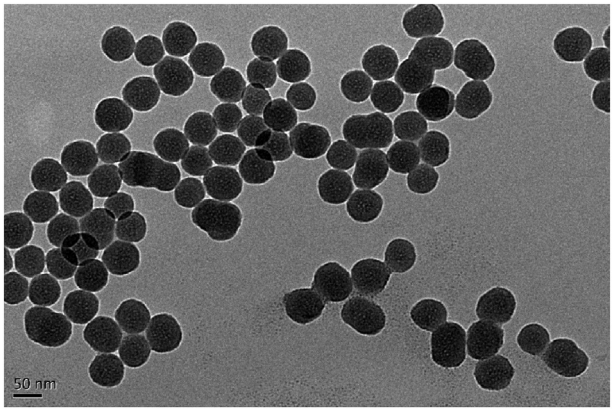

Fig. 1. Morphological image of detected SiNPs under TEM. All particles had a near-spherical shape, and dispersed well. The scale bar, 50 nm.

3.6. SiNPs enhanced oxLDL-induced ER stress response in RAW264.7 cells

Under ER stress, GRP78/BiP (binding immunoglobulin protein) was displaced from the stress sensors PERK (protein kinase RNA-like ER kinase), IRE1 (inositol-requiring endonuclease 1), and ATF6 (activating transcription factor-6) in the ER lumen, finally leading to the activation of three signaling pathways: PERK/eIF2α (eukaryotic translation initiation factor 2α), IRE1/XBP1 (X-box binding protein-1) and ATF6 pathways. Therefore, the expressions of the key indicators of ER stress were detected. As seen in Fig. 6, oxLDL remarkably triggered the expressions of three-key ER stress markers, GRP78/BiP, CHOP and XBP1S, which were all further significantly upregulated when co-exposed to SiNPs. Meantime, the expression of ER stress-associated apoptotic executor, Caspase-12 was increased after oxLDL or SiNPs exposure, and became even higher upon their co-exposure condition. Results of the three key ER stress signaling showed that protein expressions of p-PERK (the active form of PERK), p-IRE1α (the active form of IRE1α), and also mRNA expressions of ATF4 and homocysteine-inducible, endoplasmic reticulum stress-inducible, ubiquitin-like domain member 1 (HERPUD1) were all increased in oxLDL-treated RAW264.7 cells, and further significantly upregulated when co-exposed to SiNPs (Fig. 7). As compared with the control group, oxLDL induced a slight increase in the expression of p-eIF2α (the active form of eIF2α), but with no statistical significance. Nevertheless, its expression was remarkably increased when co-exposed to SiNPs. No significant alteration on ATF6 mRNA was shown in our study. Besides, results acquired from LSCM observation confirmed that after SiNPs or oxLDL plus SiNPs co-exposure, the intracellular calcium (Ca^{2+}) levels reflected by the fluorescent intensity of Fluo-3 AM were enhanced in macrophages (Fig. 8). All these data indicated that SiNPs enhanced oxLDL-induced ER stress in Raw264.7 cells.

4. Discussion

Atherosclerosis as a major pathological basis of CVD, results from a combination of abnormalities in lipoprotein metabolism, oxidative stress, chronic inflammation, and susceptibility to thrombosis. Hyperlipidemia affects millions of people worldwide, and has been reported as an independent risk factor for CVD. People with hyperlipidemia have elevated levels of serum cholesterol and an increased risk of thrombosis and atherosclerosis. Oxidation of LDL results in the generation of oxidized LDL, oxLDL, a heterogeneous mixture of oxidized lipid and proteins. Accumulative epidemiological studies have confirmed that oxLDL level is the marker of lipoprotein abnormalities, and a potential early marker for CVD (Ramos-Arellano et al., 2014). oxLDL contributes to the development of a pro-thrombotic state, and oxLDL in the arterial wall is central to the pathogenesis of atherosclerosis. Recently, the exponential growth in production and application of engineered nanomaterials/NPs inevitably brings potentially environmental and human exposure. By analogy with PM, cumulative studies have suggested that exposure to engineered NPs could induce adverse cardiovascular effects (Donaldson et al., 2013). Notably, serum lipoprotein abnormalities were involved in the NPs-induced progression of atherosclerosis (El-Hussainy el et al., 2016; Yan et al., 2017). Macrophage is the major cell for plaque progression, and its-derived foam cell is central in the pathophysiology of atherosclerosis. To date, the effects of NPs on macrophage lipid metabolism and apoptosis are poorly understood, especially under hyperlipidemia condition. Therefore, the investigation of adverse effects of SiNPs and oxLDL coexposure on macrophage-derived lipid metabolism, foam cell and apoptosis would provide guide for the prevention and control of cardiovascular diseases.

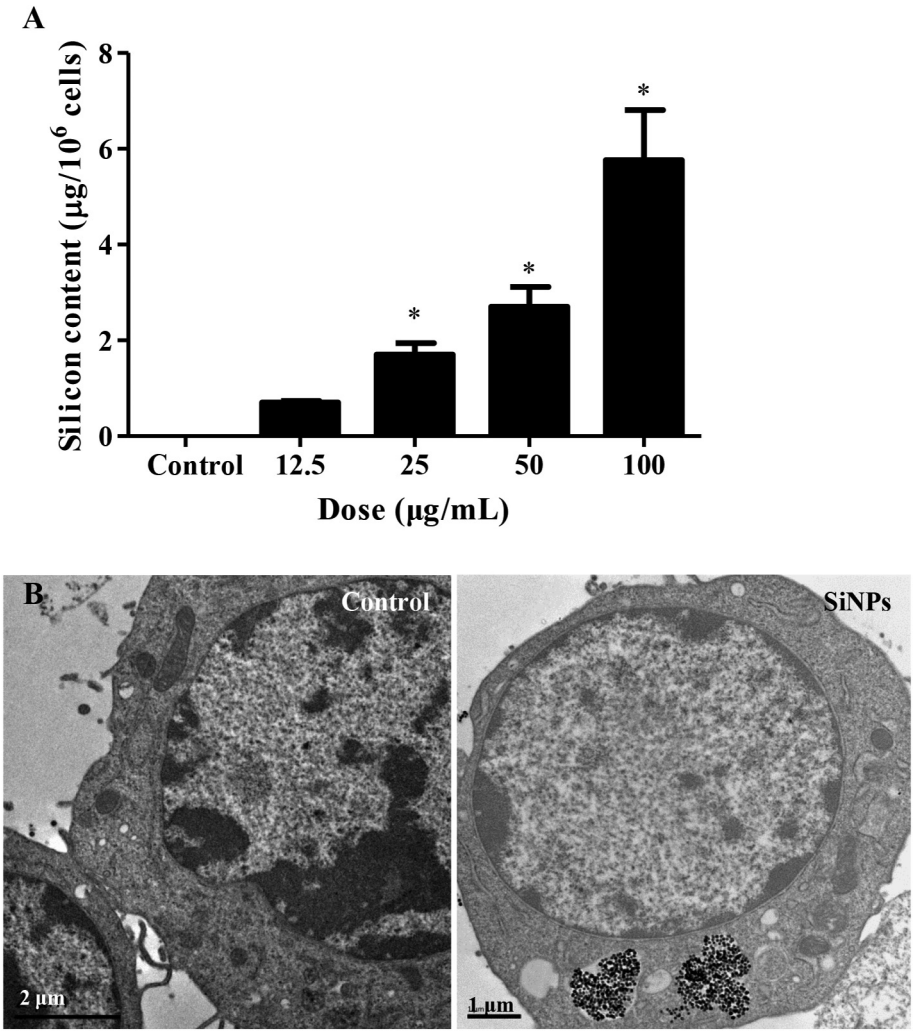

Fig. 2. SiNPs cellular uptake in Raw264.7 macrophage cells. (A) ICP-AES measurements of intracellular silicon content in macrophage, which revealed a dose-dependent SiNPs cellular uptake in Raw264.7 cells. Data are expressed as the mean ± S.D. of at least three independent experiments. $^{*}P < 0.05$ vs control. (B) Visualization of intracellular nanoparticle uptake in macrophage cells exposed to 50 μg/mL SiNPs for 24 h. Scale bar 1.0 or 2.0 μm.

In the present study, our primary results showed that oxLDL treatment resulted in macrophage injury as assessed by decreased cell viability and elevated LDH leakage and increased apoptosis. That was consistent with previous study (Yao et al., 2017). Moreover, oxLDL can be easily uptake by macrophage, and then the marked accumulation of cholesterol converts macrophages to foam cell, which could be well manifested in our findings acquired by Oil red staining and cellular TC measurement (Fig. 5). Foldbjerg et al. revealed that among the biological effects induced by SiNPs, the disturbance on lipid/cholesterol metabolism and biosynthesis were crucial (Foldbjerg et al., 2013). As for the effects on macrophage foam cell formation or lipid content induced by NPs, some in vitro studies addressed a promotion effect of NPs on macrophage foam cell formation, but the molecular mechanism was controversial (Cao et al., 2016). As early as in 2007, Niwa et al. had reported

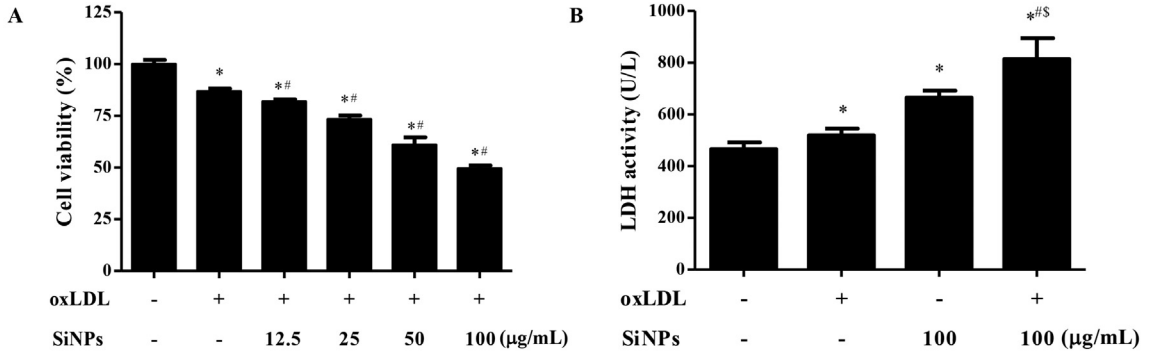

Fig. 3. SiNPs aggravated oxLDL-induced cytotoxicity in RAW264.7 cells. Cells were treated with oxLDL (25 μg/mL) in the absence or presence of SiNPs for 24 h, and the cell viability was determined by MTT assay (A), and also LDH activity in cell media was quantified (B). Data are expressed as the mean ± S.D. of at least three independent experiments. $^{*}P < 0.05$ vs control; $^{\#}P < 0.05$ vs oxLDL group; $^{\$}P < 0.05$ vs SiNPs treatment.

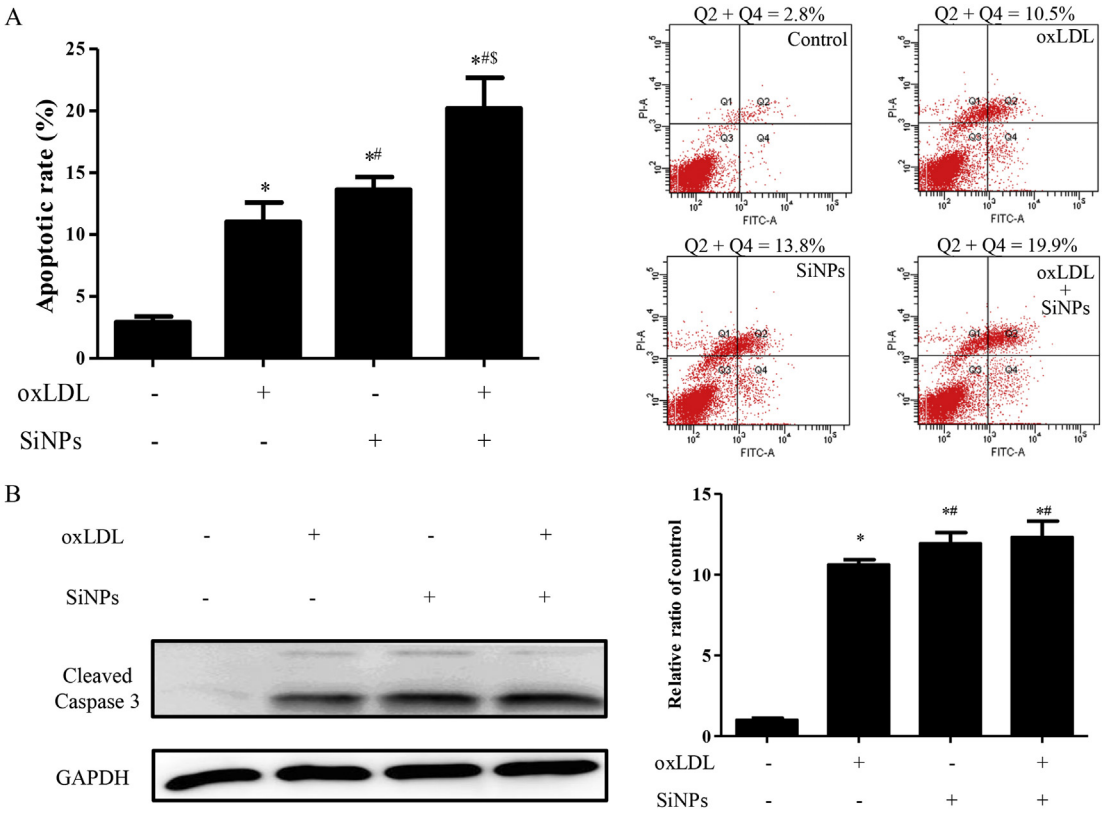

Fig. 4. SiNPs promoted oxLDL-induced apoptosis in RAW264.7 cells. Cells were treated with oxLDL (25 μg/mL) in the absence or presence of 100 μg/mL SiNPs for 24 h, then apoptosis was quantified by flow cytometry with FITC-conjugated Annexin V/propidium iodide (PI) double-staining assay (A), and also expression of cleaved caspase-3, an executor of apoptosis, was determined by Western blot and the relative densitometric analysis was performed (B). Data are expressed as the mean ± S.D. of at least three independent experiments. $^{*}P < 0.05$ vs control; $^{\#}P < 0.05$ vs oxLDL group; $^{\$}P < 0.05$ vs SiNPs treatment.

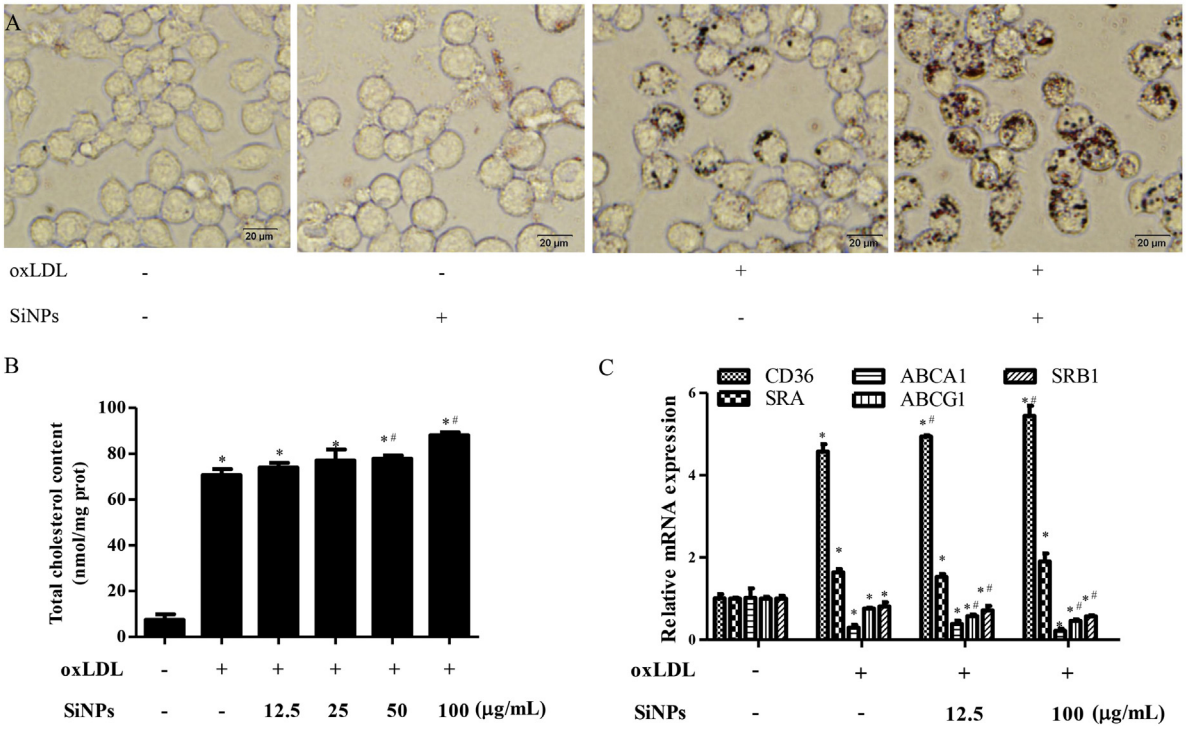

Fig. 5. SiNPs enhanced oxLDL-induced intracellular lipid accumulation in RAW264.7 cells. Cells were treated with oxLDL (25 μg/mL) in the absence or presence of 100 μg/mL SiNPs for 24 h, and the intracellular lipid droplets were stained by oil red O. Representative lipid droplet staining images are shown (A). Scale bar = 20 μm. (B) Under the similar conditions as in (A), the intracellular total cholesterol (TC) contents were measured using a tissue/cell TC assay kit. Moreover, the relative mRNA expressions of key factors involved in cholesterol efflux/influx were quantified using real-time PCR (C). Data are expressed as the mean ± S.D. of at least three independent experiments. $^{*}P < 0.05$ vs control; $^{\#}P < 0.05$ vs oxLDL treatment.

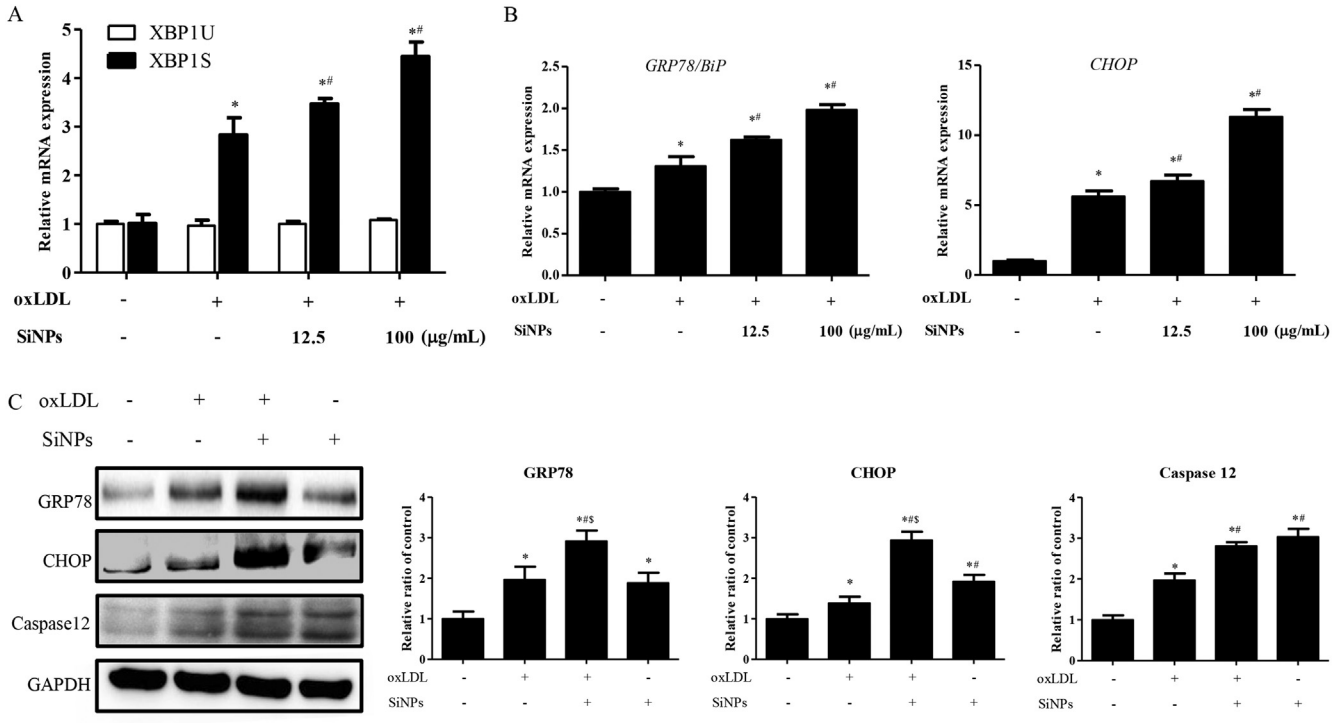

Fig. 6. SiNPs enhanced oxLDL-induced ER stress response in Raw264.7 cells. (A) XBP1 splicing and (B) the up-regulated transcription of GRP78/BiP and CHOP induced by oxLDL (25 μg/mL) in the absence or presence of SiNPs for 24 h. Moreover, when cells were treated with oxLDL (25 μg/mL) in the absence or presence of 100 μg/mL SiNPs for 24 h, the protein expressions of GRP78/BiP and CHOP, as well as Caspase-12 were detected by Western blot (C). Data are expressed as the mean ± S.D. of at least three independent experiments. $^{*}P < 0.05$ vs control; $^{\#}P < 0.05$ vs oxLDL group; $^{\$}P < 0.05$ vs SiNPs treatment.

that engineered nanomaterials (water-soluble fullerene and carbon black) induced oxLDL cellular uptake and foam cell-like formation (Niwa and Iwai, 2007). Here, we firstly reported SiNPs induced macrophages to uptake oxLDL and become foam cell in vitro (Fig. 5A). In line with our study, Petrick et al. observed a modest increase in cholesterol mass and a significant increase in triglyceride content on SiNPs-exposed macrophages, and also a colocalization of SiNPs with lipid droplets in macrophages (Petrick et al., 2016). But no in-depth molecular mechanistic investigation was included in their study. It was previously showed that some metallic NPs could induce lipid droplet formation, and co-localization of lipid droplets with lysosomes was also observed (Khatchadourian and Maysinger, 2009). Besides lipid droplets, the amorphous SiNPs were mainly accumulated in lysosomes of macrophages (Hashimoto and Imazato, 2015), which cause the lysosomes to become enlarged even like a balloon under TEM observation. To be noted, we only observed an internalization of SiNPs in macrophages at the present study (Fig. 2B), but a more accurate intracellular location of SiNPs was not included, which might limit our explanation of observed promoting effects of SiNPs on lipid accumulation and foam cell formation. Otherwise, interestingly, TiO_2 NPs penetrated lipid droplets, but it was suspected to cause the decrease in intracellular lipid accumulation (Xu et al., 2017). To date, there is no in vivo evidence for the macrophage foam cell formation in the atherosclerotic plaques after engineered NPs exposure. Certain previous studies have demonstrated that SiNPs could increase apoptosis of Raw264.7 macrophage cells (Duan et al., 2016; Wilhelmi et al., 2012), and even cause DNA damage (Duan et al., 2016; Hashimoto and Imazato, 2015). Bioinformatics analysis done by Zhang et al. found that the majority of differentially expressed genes in SiNPs-treated Raw264.7 cells were mainly involved in the regulation of macrophage apoptosis, inflammatory response and cell differentiation (Zhang et al., 2017), indicating macrophage apoptosis as one of the most important cellular process affected by exposure to SiNPs. Further, our finding showed that SiNPs enhanced oxLDL-induced effects on the toxicity, lipid uptake and even apoptosis of macrophages, implying a more deleterious influence when human facing the coexistence of hyperlipidemia and NPs pollution. Since hyperlipidemia and NPs exposure are common worldwidely, more detailed investigations related to the interaction between hyperlipidemia and NPs are needed, and further research on the exact mechanism is urgently warranted for exploration.

ER is an important organelle which regulates calcium homeostasis, protein synthesis and modification, especially lipid production, metabolism, post-translational modification and trafficking. A large body of evidence suggests a connection between ER stress and lipid homeostasis (Zhang et al., 2016; Zhou et al., 2016). Prolonged or overwhelming ER stress induced abnormal lipid metabolism through a transcriptional regulation of lipogenesis and also a inhibition of lipid degradation (Zhao et al., 2010), contributing to many human disorders, including dyslipidemia, insulin resistance, diabetes, obesity, and even cancer. Meanwhile, severe ER stress could trigger macrophage apoptosis, in turn resulting in plaque necrosis (Tsukano et al., 2010). Both humans and animal evidence confirmed ER stress markers were enhanced in atherosclerotic lesions, and ER stress and associated apoptosis were correlated with plaque instability and rupture in atherosclerosis (Ivanova and Orekhov, 2016). To date, ER stress (also known as unfolded protein response, UPR) has mainly three signaling pathways by stress sensors: PERK/eIF2α/ATF4, IRE1α/XBP1, and ATF6. Normally, the three stress-sensing proteins (PERK, IRE1 and ATF6) are held in inactive state by ER-chaperone protein GRP78/BiP. Under ER stress condition, the dissociation of GRP78/BiP from any of the three ER stress sensors results in the activation of the three different UPR signaling pathways. IRE1 mediates XBP1 splicing (a removal of 26 nucleotides long intron from *XBP1* mRNA and introducing a frame-shift and an alternative C-terminus in the spliced form, *XBP1S*). Generally, the induction of GRP78/*BiP* transcription and *XBP1* splicing are frequently used as specific markers of ER stress response (van Schadewijk et al., 2012). It has been well demonstrated that ER stress participates in the harmful effects of oxLDL in many types of cells (Hong et al., 2014; Plaisance et al., 2016). Indeed,

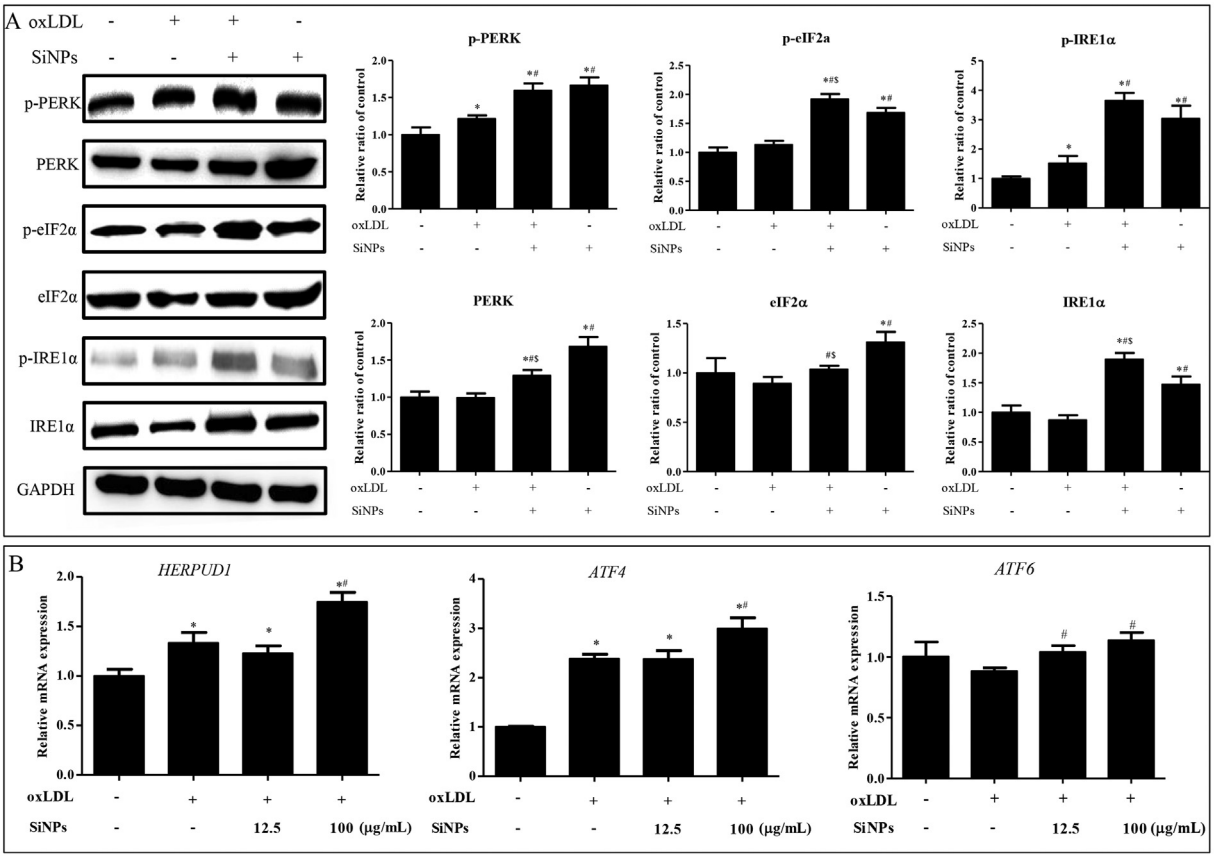

Fig. 7. SiNPs enhanced oxLDL-induced activation of ER stress signaling pathway in Raw264.7 cells. Cells were treated with oxLDL (25 μg/mL) in the absence or presence of 100 μg/mL SiNPs for 24 h, and the protein expressions of key factors involved in ER stress signaling pathways, including PERK, p-PERK, eIF2α, p-eIF2α, IRE1α, p-IRE1α were detected by Western blot, and their relative densitometric analysis were preformed and presented. (B) Under the similar conditions as in (A), the mRNA expressions of HERPUD1, ATF4 and ATF6 were quantified by real-time PCR. Data are expressed as the mean ± S.D. of at least three independent experiments. $^{*}P < 0.05$ vs control; $^{\#}P < 0.05$ vs oxLDL group; $^{\$}P < 0.05$ vs SiNPs treatment.

we observed up-regulated GRP78 and CHOP expressions (in both mRNA and protein levels) and *XBP1* splicing in the oxLDL-treated macrophages (Fig. 6). Furthermore, as the results indicated, two out of the three branches of ER stress signaling (PERK/eIF2α/ATF4 and IRE1α/XBP1) were triggered by oxLDL. We detected no significant alteration on ATF6 mRNA level in macrophages after oxLDL treatment; whereas Yao et al. reported ER stress-related proteins, particularly ATF6 and CHOP, were involved in oxLDL-induced cholesterol accumulation and apoptosis in macrophages (Yao et al., 2013). That might be associated with a relative lower dose of oxLDL (25 μg/mL) used in our study. At the meantime, another important ER stress marker gene HERPUD1 was remarkably increased after oxLDL treatment, indicating an accumulation of the unfolded proteins in ER. In addition, the elevation of cytosolic Ca^{2+} level is known as a typical ER stress response of cells (Krebs et al., 2015). Actually, a slightly increased Ca^{2+} level was observed after oxLDL treatment (Fig. 8). Reportedly, the cytosolic Ca^{2+} overload would be followed by uptake of Ca^{2+} into mitochondrion, leading to mitochondrial injury and ultimately apoptosis (Bhandary et al., 2012; Deniaud et al., 2008). Recently, ER stress and NPs exposure had been well reviewed (Cao et al., 2017). A large body of evidence suggested ER stress could be the mechanisms responsible for NPs-induced toxicity. Modulation of ER stress by NPs could be a potential way for disease therapy, especially for cardiovascular and metabolic diseases. Moreover, the induction of ER stress could enhance the toxicity of NPs to macrophages (Chen et al., 2017). However, the induction of ER stress was varied according to the NPs or cell type under investigation. For instance, the induction of ER stress was not observed in brain microvascular endothelial cells upon the different-sized gold NPs modified with various polymers (Anspach et al., 2016). Here, similar to oxLDL, a trigger of ER stress in macrophages was induced by SiNPs as evidenced by

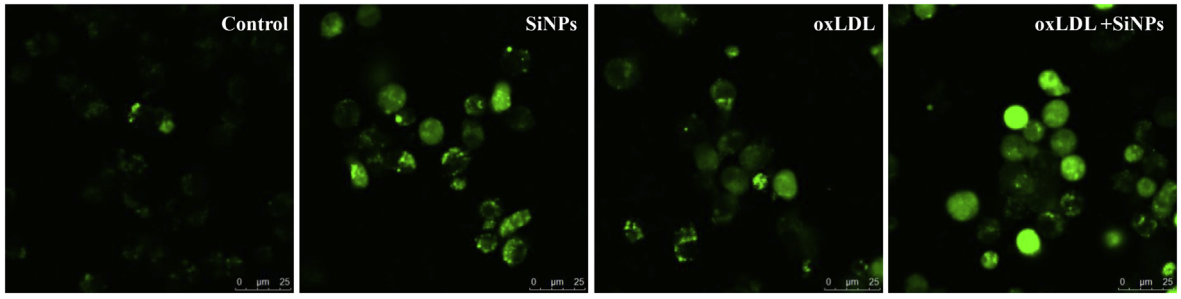

Fig. 8. SiNPs enhanced oxLDL-induced cytosolic calcium overload in Raw264.7 cells. Cells were treated with oxLDL (25 μg/mL) in the absence or presence of 100 μg/mL SiNPs for 24 h, and the intracellular calcium level was detected using Ca^{2+}-specific fluorescent dye, Fluo-3 AM. The representative LSCM image showed an enhancement of cytosolic calcium in macrophages after SiNPs or oxLDL treatment, especially upon SiNPs and oxLDL coexposure condition. Scale bar = 25 μm.

GRP78 and CHOP upregulation, and also the activation of PERK/eIF2α and IRE1α signaling. In line with our study, SiNPs perturbated the ER, leading to the ER stress response in human liver line Huh7, as well as silver-coated SiNPs (Christen and Fent, 2012; Christen and Fent, 2016). Under the oxLDL and SiNPs co-exposure condition, the observed ER stress responses were all enhanced when compared with the oxLDL treatment group. Therefore, SiNPs enhanced the oxLDL-triggered activation of ER stress signaling, implying a vital role of ER stress in the observed macrophage toxicity upon SiNPs and oxLDL coexposure.

The intracellular cholesterol homeostasis in mammalian cells was highly, precisely regulated by cholesterol influx and efflux. An interrupt of this balance would fuel atherogenesis. oxLDL could be trafficked by the scavenger receptors of macrophage (CD36, SRA1) to the ER in the cytoplasm, while the accumulation of toxic lipids in macrophages can lead to a prolonged ER stress. Moreover, ER stress could modulate cholesterol homeostasis through promoting cholesterol influx and impairing cholesterol efflux via regulating the expressions of CD36 (Hua et al., 2010; Yao et al., 2014), also ABCA1 (Castilho et al., 2012) on macrophages, and thus promoted macrophage-derived foam cell formation and apoptosis (Yao et al., 2014). That could well explain our observation on up-regulated expressions on CD36 and SRA, and down-regulated expressions on ABCA1, ABCG1 and SRB1 upon oxLDL and SiNPs coexposure. The impairment on membrane integrity, as indicated by the increase in LDH release upon oxLDL and SiNPs coexposure, might be an important reason for the inhibition of ABC efflux transporters (Liu et al., 2016). Similarly, NPs exposure has been shown to induce the expression of scavenger receptors by several investigators (Shannahan et al., 2015; Suzuki et al., 2014). Additionally, ER stress-mediated NPs-induced apoptosis in many cell types has been well elucidated recently (Cao et al., 2017). CHOP transcription factor is up-regulated after ER stress, and can initiate apoptotic cell death through triggering a Ca^{2+} release from ER (Tabas, 2010). Capase-12 is regarded as an executor of ER stress-mediated apoptotic event (Urano et al., 2000). Our findings about the activation of CHOP and Caspase-12 implied the detected apoptosis induced by oxLDL or SiNPs was mediated by an ER stress-dependent way. The induction of CHOP indicated an increase in ER-initiated apoptosis, while that of GRP78 represented for the adaptive response, which suppressed apoptosis (Yao et al., 2013). ER stress may act as a protective role initially, but prolonged ER stress would lead to macrophage apoptosis. Reportedly, inhibition of ER stress could effectively reverse the oxLDL-mediated formation and apoptosis of macrophage-derived foam cell (Tian et al., 2015; Yao et al., 2015). In this context, ER stress may participate in the oxLDL- or SiNPs-induced accumulation of cholesterol in the cytoplasm, and finally foam cell formation and apoptosis.

5. Conclusion

In summary, our results showed that oxLDL-incubated macrophages displayed the declined cell viability, increased apoptosis, caspase-3 activation, and cellular cholesterol level, and activation of ER stress, which were all augmented by SiNPs coexposure. These results implied that SiNPs markedly enhanced oxLDL-triggered lipid accumulation and apoptosis of macrophages via triggering ER stress signaling pathway. To our best knowledge, our study firstly revealed the induction of foam cell along with the disturbance on cholesterol influx/efflux balance, and promotion of apoptosis via ER stress PERK/eIF2α/ATF4 and IRE1α/XBP1 signaling cascade by SiNPs and oxLDL coexposure in a macrophage model. Our findings may provide an in vitro evidence for atherogenic properties of SiNPs, and also offer essential information for a better understanding of the toxicity or interaction of hyperlipidemia and NPs coexposure.

Supplementary data to this article can be found online at https://doi.org/10.1016/j.scitotenv.2018.02.312.

Conflict of interest

There is no actual or potential conflict of interests.

Acknowledgments

The work was supported by the National Natural Science Foundation of China (81102095, 81230065), Beijing Natural Science Foundation Program (7162021), and Beijing Education Committee Program for Cultivation of Young Top-notch Personnel in Beijing Municipality (CIT&TCD201804090).

References

Anspach, L., Unger, R.E., Brochhausen, C., Gibson, M.I., Klok, H.A., Kirkpatrick, C.J., et al., 2016. Impact of polymer-modified gold nanoparticles on brain endothelial cells: exclusion of endoplasmic reticulum stress as a potential risk factor. Nanotoxicology 10, 1341–1350.
Arai, H., 2014. Oxidative modification of lipoproteins. Subcell. Biochem. 77, 103–114.
Asweto, C.O., Wu, J., Hu, H., Feng, L., Yang, X., Duan, J., et al., 2017. Combined effect of silica nanoparticles and benzo[a]pyrene on cell cycle arrest induction and apoptosis in human umbilical vein endothelial cells. Int. J. Environ. Res. Public Health 14.
Bhandary, B., Marahatta, A., Kim, H.R., Chae, H.J., 2012. An involvement of oxidative stress in endoplasmic reticulum stress and its associated diseases. Int. J. Mol. Sci. 14, 434–456.
Bobryshev, Y.V., Ivanova, E.A., Chistiakov, D.A., Nikiforov, N.G., Orekhov, A.N., 2016. Macrophages and their role in atherosclerosis: pathophysiology and transcriptome analysis. Biomed. Res. Int. 2016, 9582430.
Breznan, D., Das, D.D., O'Brien, J.S., MacKinnon-Roy, C., Nimesh, S., Vuong, N.Q., et al., 2017. Differential cytotoxic and inflammatory potency of amorphous silicon dioxide nanoparticles of similar size in multiple cell lines. Nanotoxicology 11, 223–235.
Brook, R.D., Newby, D.E., Rajagopalan, S., 2017. Air pollution and cardiometabolic disease: an update and call for clinical trials. Am. J. Hypertens. 31, 1–10.
Cao, Y., Long, J., Ji, Y., Chen, G., Shen, Y., Gong, Y., et al., 2016. Foam cell formation by particulate matter (PM) exposure: a review. Inhal. Toxicol. 28, 583–590.
Cao, Y., Long, J., Liu, L., He, T., Jiang, L., Zhao, C., et al., 2017. A review of endoplasmic reticulum (ER) stress and nanoparticle (NP) exposure. Life Sci. 186, 33–42.
Castilho, G., Okuda, L.S., Pinto, R.S., Iborra, R.T., Nakandakare, E.R., Santos, C.X., et al., 2012. ER stress is associated with reduced ABCA-1 protein levels in macrophages treated with advanced glycated albumin - reversal by a chemical chaperone. Int. J. Biochem. Cell Biol. 44, 1078–1086.
Chang, C.Y., Shen, C.Y., Kang, C.K., Sher, Y.P., Sheu, W.H., Chang, C.C., et al., 2014. Taurine protects HK-2 cells from oxidized LDL-induced cytotoxicity via the ROS-mediated mitochondrial and p53-related apoptotic pathways. Toxicol. Appl. Pharmacol. 279, 351–363.
Chen, G., Shen, Y., Li, X., Jiang, Q., Cheng, S., Gu, Y., et al., 2017. The endoplasmic reticulum stress inducer thapsigargin enhances the toxicity of ZnO nanoparticles to macrophages and macrophage-endothelial co-culture. Environ. Toxicol. Pharmacol. 50, 103–110.
Christen, V., Fent, K., 2012. Silica nanoparticles and silver-doped silica nanoparticles induce endoplasmatic reticulum stress response and alter cytochrome P4501A activity. Chemosphere 87, 423–434.
Christen, V., Fent, K., 2016. Silica nanoparticles induce endoplasmic reticulum stress response and activate mitogen activated kinase (MAPK) signalling. Toxicol. Rep. 3, 832–840.
Deniaud, A., Sharaf el dein, O., Maillier, E., Poncet, D., Kroemer, G., Lemaire, C., et al., 2008. Endoplasmic reticulum stress induces calcium-dependent permeability transition, mitochondrial outer membrane permeabilization and apoptosis. Oncogene 27, 285–299.
Donaldson, K., Duffin, R., Langrish, J.P., Miller, M.R., Mills, N.L., Poland, C.A., et al., 2013. Nanoparticles and the cardiovascular system: a critical review. Nanomedicine (London) 8, 403–423.
Du, Z., Zhao, D., Jing, L., Cui, G., Jin, M., Li, Y., et al., 2013. Cardiovascular toxicity of different sizes amorphous silica nanoparticles in rats after intratracheal instillation. Cardiovasc. Toxicol. 13, 194–207.
Duan, J., Kodali, V.K., Gaffrey, M.J., Guo, J., Chu, R.K., Camp, D.G., et al., 2016. Quantitative profiling of protein S-glutathionylation reveals redox-dependent regulation of macrophage function during nanoparticle-induced oxidative stress. ACS Nano 10, 524–538.
El-Hussainy el, H.M., Hussein, A.M., Abdel-Aziz, A., El-Mehasseb, I., 2016. Effects of aluminum oxide (Al2O3) nanoparticles on ECG, myocardial inflammatory cytokines, redox state, and connexin 43 and lipid profile in rats: possible cardioprotective effect of gallic acid. Can. J. Physiol. Pharmacol. 94, 868–878.
Foldbjerg, R., Wang, J., Beer, C., Thorsen, K., Sutherland, D.S., Autrup, H., 2013. Biological effects induced by BSA-stabilized silica nanoparticles in mammalian cell lines. Chem. Biol. Interact. 204, 28–38.
Guo, C., Xia, Y., Niu, P., Jiang, L., Duan, J., Yu, Y., et al., 2015. Silica nanoparticles induce oxidative stress, inflammation, and endothelial dysfunction in vitro via activation of the MAPK/Nrf2 pathway and nuclear factor-kappaB signaling. Int. J. Nanomedicine 10, 1463–1477.
Guo, C., Yang, M., Jing, L., Wang, J., Yu, Y., Li, Y., et al., 2016. Amorphous silica nanoparticles trigger vascular endothelial cell injury through apoptosis and autophagy via reactive

oxygen species-mediated MAPK/Bcl-2 and PI3K/Akt/mTOR signaling. Int. J. Nanomedicine 11, 5257–5276.
Guo, C., Wang, J., Jing, L., Ma, R., Liu, X., Gao, L., et al., 2018. Mitochondrial dysfunction, perturbations of mitochondrial dynamics and biogenesis involved in endothelial injury induced by silica nanoparticles. Environ. Pollut. 236, 926–936.
Hashimoto, M., Imazato, S., 2015. Cytotoxic and genotoxic characterization of aluminum and silicon oxide nanoparticles in macrophages. Dent. Mater. 31, 556–564.
Hong, D., Bai, Y.P., Gao, H.C., Wang, X., Li, L.F., Zhang, G.G., et al., 2014. Ox-LDL induces endothelial cell apoptosis via the LOX-1-dependent endoplasmic reticulum stress pathway. Atherosclerosis 235, 310–317.
Hua, Y., Kandadi, M.R., Zhu, M., Ren, J., Sreejayan, N., 2010. Tauroursodeoxycholic acid attenuates lipid accumulation in endoplasmic reticulum-stressed macrophages. J. Cardiovasc. Pharmacol. 55, 49–55.
Ivanova, E.A., Orekhov, A.N., 2016. The role of endoplasmic reticulum stress and unfolded protein response in atherosclerosis. Int. J. Mol. Sci. 17.
Khatchadourian, A., Maysinger, D., 2009. Lipid droplets: their role in nanoparticle-induced oxidative stress. Mol. Pharm. 6, 1125–1137.
Krebs, J., Agellon, L.B., Michalak, M., 2015. Ca(2+) homeostasis and endoplasmic reticulum (ER) stress: an integrated view of calcium signaling. Biochem. Biophys. Res. Commun. 460, 114–121.
Li, Q., Wu, H., Yue, W., Dai, Q., Liang, H., Bian, H., et al., 2017. Prevalence of stroke and vascular risk factors in China: a nationwide community-based study. Sci. Rep. 7, 6402.
Linton, M.F., Yancey, P.G., Davies, S.S., Jerome, W.G.J., Linton, E.F., Vickers, K.C., 2000. The Role of Lipids and Lipoproteins in Atherosclerosis.
Linton, M.F., Babaev, V.R., Huang, J., Linton, E.F., Tao, H., Yancey, P.G., 2016. Macrophage apoptosis and efferocytosis in the pathogenesis of atherosclerosis. Circ. J. 80, 2259–2268.
Liu, X., Sun, J.A., 2010. Endothelial cells dysfunction induced by silica nanoparticles through oxidative stress via JNK/P53 and NF-kappa B pathways. Biomaterials 31, 8198–8209.
Liu, X., Xue, Y., Ding, T., Sun, J., 2012. Enhancement of proinflammatory and procoagulant responses to silica particles by monocyte-endothelial cell interactions. Part. Fibre Toxicol. 9, 36.
Liu, S., Jiang, W., Wu, B., Yu, J., Yu, H., Zhang, X.X., et al., 2016. Low levels of graphene and graphene oxide inhibit cellular xenobiotic defense system mediated by efflux transporters. Nanotoxicology 10, 597–606.
Lu, C.F., Yuan, X.Y., Li, L.Z., Zhou, W., Zhao, J., Wang, Y.M., et al., 2015. Combined exposure to nano-silica and lead induced potentiation of oxidative stress and DNA damage in human lung epithelial cells. Ecotoxicol. Environ. Saf. 122, 537–544.
Matsuo, K., Hirobe, S., Okada, N., Nakagawa, S., 2016. Analysis of skin permeability and toxicological properties of amorphous silica particles. Biol. Pharm. Bull. 39, 1201–1205.
May, J.M., Qu, Z.C., 2010. Ascorbic acid prevents increased endothelial permeability caused by oxidized low density lipoprotein. Free Radic. Res. 44, 1359–1368.
Miller, M.R., Raftis, J.B., Langrish, J.P., McLean, S.G., Samutrtai, P., Connell, S.P., et al., 2017. Inhaled nanoparticles accumulate at sites of vascular disease. ACS Nano 11, 4542–4552.
Murugadoss, S., Lison, D., Godderis, L., Van Den Brule, S., Mast, J., Brassinne, F., et al., 2017. Toxicology of silica nanoparticles: an update. Arch. Toxicol. 91, 2967–3010.
Napierska, D., Quarck, R., Thomassen, L.C., Lison, D., Martens, J.A., Delcroix, M., et al., 2013. Amorphous silica nanoparticles promote monocyte adhesion to human endothelial cells: size-dependent effect. Small 9, 430–438.
Nemmar, A., Albarwani, S., Beegam, S., Yuvaraju, P., Yasin, J., Attoub, S., et al., 2014. Amorphous silica nanoparticles impair vascular homeostasis and induce systemic inflammation. Int. J. Nanomedicine 9, 2779–2789.
Nemmar, A., Yuvaraju, P., Beegam, S., Yasin, J., Kazzam, E.E., Ali, B.H., 2016. Oxidative stress, inflammation, and DNA damage in multiple organs of mice acutely exposed to amorphous silica nanoparticles. Int. J. Nanomedicine 11, 919–928.
Nishi, K., Itabe, H., Uno, M., Kitazato, K.T., Horiguchi, H., Shinno, K., et al., 2002. Oxidized LDL in carotid plaques and plasma associates with plaque instability. Arterioscler. Thromb. Vasc. Biol. 22, 1649–1654.
Niwa, Y., Iwai, N., 2007. Nanomaterials induce oxidized low-density lipoprotein cellular uptake in macrophages and platelet aggregation. Circ. J. 71, 437–444.
Petrick, L., Rosenblat, M., Paland, N., Aviram, M., 2016. Silicon dioxide nanoparticles increase macrophage atherogenicity: stimulation of cellular cytotoxicity, oxidative stress, and triglycerides accumulation. Environ. Toxicol. 31, 713–723.
Plaisance, V., Brajkovic, S., Tenenbaum, M., Favre, D., Ezanno, H., Bonnefond, A., et al., 2016. Endoplasmic reticulum stress links oxidative stress to impaired pancreatic beta-cell function caused by human oxidized LDL. PLoS One 11, e0163046.
Ramos-Arellano, L.E., Munoz-Valle, J.F., De la Cruz-Mosso, U., Salgado-Bernabe, A.B., Castro-Alarcon, N., Parra-Rojas, I., 2014. Circulating CD36 and oxLDL levels are associated with cardiovascular risk factors in young subjects. BMC Cardiovasc. Disord. 14, 54.
Roth, G.A., Johnson, C., Abajobir, A., Abd-Allah, F., Abera, S.F., Abyu, G., et al., 2017. Global, regional, and National Burden of cardiovascular diseases for 10 causes, 1990 to 2015. J. Am. Coll. Cardiol. 70, 1–25.
van Schadewijk, A., van't Wout, E.F., Stolk, J., Hiemstra, P.S., 2012. A quantitative method for detection of spliced X-box binding protein-1 (XBP1) mRNA as a measure of endoplasmic reticulum (ER) stress. Cell Stress Chaperones 17, 275–279.
Shannahan, J.H., Sowrirajan, H., Persaud, I., Podila, R., Brown, J.M., 2015. Impact of silver and iron nanoparticle exposure on cholesterol uptake by macrophages. J. Nanomater. 2015, 1–12.
Suzuki, Y., Tada-Oikawa, S., Ichihara, G., Yabata, M., Izuoka, K., Suzuki, M., et al., 2014. Zinc oxide nanoparticles induce migration and adhesion of monocytes to endothelial cells and accelerate foam cell formation. Toxicol. Appl. Pharmacol. 278, 16–25.
Tabas, I., 2010. The role of endoplasmic reticulum stress in the progression of atherosclerosis. Circ. Res. 107, 839–850.
Tay, C.Y., Setyawati, M.I., Leong, D.T., 2017. Nanoparticle density: a critical biophysical regulator of endothelial permeability. ACS Nano 11, 2764–2772.
Tian, H., Sun, H.W., Zhang, J.J., Zhang, X.W., Zhao, L., Guo, S.D., et al., 2015. Ethanol extract of propolis protects macrophages from oxidized low density lipoprotein-induced apoptosis by inhibiting CD36 expression and endoplasmic reticulum stress-C/EBP homologous protein pathway. BMC Complement. Altern. Med. 15, 230.
Traboulsi, H., Guerrina, N., Iu, M., Maysinger, D., Ariya, P., Baglole, C.J., 2017. Inhaled pollutants: the molecular scene behind respiratory and systemic diseases associated with ultrafine particulate matter. Int. J. Mol. Sci. 18.
Tsukano, H., Gotoh, T., Endo, M., Miyata, K., Tazume, H., Kadomatsu, T., et al., 2010. The endoplasmic reticulum stress-C/EBP homologous protein pathway-mediated apoptosis in macrophages contributes to the instability of atherosclerotic plaques. Arterioscler. Thromb. Vasc. Biol. 30, 1925–1932.
Urano, F., Wang, X., Bertolotti, A., Zhang, Y., Chung, P., Harding, H.P., et al., 2000. Coupling of stress in the ER to activation of JNK protein kinases by transmembrane protein kinase IRE1. Science 287, 664–666.
Wilhelmi, V., Fischer, U., van Berlo, D., Schulze-Osthoff, K., Schins, R.P., Albrecht, C., 2012. Evaluation of apoptosis induced by nanoparticles and fine particles in RAW 264.7 macrophages: facts and artefacts. Toxicol. in Vitro 26, 323–334.
Xu, Y., Hadjiargyrou, M., Rafailovich, M., Mironava, T., 2017. Cell-based cytotoxicity assays for engineered nanomaterials safety screening: exposure of adipose derived stromal cells to titanium dioxide nanoparticles. J. Nanobiotechnol. 15, 50.
Yan, Z., Wang, W., Wu, Y., Li, B., Liang, N., Wu, W., 2017. Zinc oxide nanoparticle-induced atherosclerotic alterations in vitro and in vivo. Int. J. Nanomedicine 12, 4433–4442.
Yao, S., Zong, C., Zhang, Y., Sang, H., Yang, M., Jiao, P., et al., 2013. Activating transcription factor 6 mediates oxidized LDL-induced cholesterol accumulation and apoptosis in macrophages by up-regulating CHOP expression. J. Atheroscler. Thromb. 20, 94–107.
Yao, S., Miao, C., Tian, H., Sang, H., Yang, N., Jiao, P., et al., 2014. Endoplasmic reticulum stress promotes macrophage-derived foam cell formation by up-regulating cluster of differentiation 36 (CD36) expression. J. Biol. Chem. 289, 4032–4042.
Yao, S., Tian, H., Miao, C., Zhang, D.W., Zhao, L., Li, Y., et al., 2015. D4F alleviates macrophage-derived foam cell apoptosis by inhibiting CD36 expression and ER stress-CHOP pathway. J. Lipid Res. 56, 836–847.
Yao, S., Tian, H., Zhao, L., Li, J., Yang, L., Yue, F., et al., 2017. Oxidized high density lipoprotein induces macrophage apoptosis via toll-like receptor 4-dependent CHOP pathway. J. Lipid Res. 58, 164–177.
Zhang, M., Yu, Q., Liang, C., Zhang, B., Li, M., 2016. Lipid homeostasis is involved in plasma membrane and endoplasmic reticulum stress in Pichia Pastoris. Biochem. Biophys. Res. Commun. 478, 777–783.
Zhang, L., Hao, C., Li, J., Qu, Y., Bao, L., Li, Y., et al., 2017. Bioinformatics methods for identifying differentially expressed genes and signaling pathways in nano-silica stimulated macrophages. Tumour Biol. 39 (1010428317709284).
Zhao, Y., Guo, Z., Lin, X., Zhou, L., Okoro, E.U., Fan, G., et al., 2010. Apolipoprotein E-deficient lipoproteins induce foam cell formation by activation of PERK-EIF-2alpha signaling Cascade. J. Bioanal. Biomed. 2, 113–120.
Zhou, L., Ding, S., Li, Y., Wang, L., Chen, W., Bo, T., et al., 2016. Endoplasmic reticulum stress may play a pivotal role in lipid metabolic disorders in a novel mouse model of subclinical hypothyroidism. Sci. Rep. 6, 31381.